Biochemistry and Biophysics Reports 13 (2018) 99–108

Contents lists available at ScienceDirect

Biochemistry and Biophysics Reports

journal homepage: www.elsevier.com/locate/bbrep

The role of the ShcD and RET interaction in neuroblastoma survival and migration

Zeanap A. Mabruk[a,*,1], Samrein B.M. Ahmed[a,*,1], Asha Caroline Thomas[a], Sally A. Prigent[b]

[a] Sharjah Institute for Medical Research and College of Medicine University of Sharjah, United Arab Emirates
[b] Department of Molecular and Cellular Biology, University of Leicester, UK

ARTICLE INFO

Keywords:
ShcD
RET
Neuroblastoma
Endosomes
GDNF

ABSTRACT

Preliminary screening data showed that the ShcD adaptor protein associates with the proto-oncogene RET receptor tyrosine kinase. In the present study, we aimed to investigate the molecular interaction between ShcD and RET in human neuroblastoma cells and study the functional impact of this interaction. We were able to show that ShcD immunoprecipitated with RET from SK-N-AS neuroblastoma cell lysates upon GDNF treatment. This result was validated by ShcD-RET co-localization, which was visualized using a fluorescence microscope. ShcD-RET coexpression promoted ShcD and RET endosomal localization, resulting in unexpected inhibition of the downstream ERK and AKT pathways. Interestingly, ShcD-RET association reduced the viability and migration of SK-N-AS cells. Although ShcD was previously shown to trigger melanoma cell migration and tumorigenesis, our data showed an opposite role for ShcD in neuroblastoma SK-N-AS cells via its association with RET in GDNF-treated cells. In conclusion, ShcD acts as a switch molecule that promotes contrasting biological responses depending on the stimulus ad cell type.

1. Introduction

Adaptor proteins are key factors in maintaining intracellular homeostasis. These proteins form a dynamic link between the receptor and effector motifs of signalling pathways, enabling cellular signals to be transduced and appropriate physiological responses to be generated [1]. Any disorder in the expression of adaptor proteins may lead to a disease condition or, in some cases, may trigger cancer formation [2]. The Src homology and collagen (Shc) family of adaptor proteins modulates the dynamics of various intracellular cascades downstream of different receptor tyrosine kinases (RTKs) through the family's various Shc isoforms, which have multiple domains [3,4]. The recently identified melanoma-associated adaptor ShcD belongs to the Shc family of adaptor proteins [5]. ShcD expression was found to be upregulated in invasive melanoma [5,6], which led researchers to propose ShcD as a therapeutic target for melanoma treatment [7].

Previous studies showed that ShcD associates with various tyrosine kinase receptors, such as muscle specific kinase receptor (MUSK), epidermal growth factor receptor (EGFR), neurotrophic receptors (TrkA/B/C), RET, anaplastic lymphoma kinase (ALK), Met, insulin growth factor-1 receptor (IGF-1 R), ErbB2/4 and vascular endothelial growth factor receptor-3 (VEGR-3 [6,8,9], albeit little has been reported regarding the consequences of ShcD-receptor interactions.

The ShcD and MUSK association was shown to interfere with acetylcholine receptor phosphorylation at the neuromuscular junction [9], while the ShcD and TrkB interaction was suggested to have a role in brain cell differentiation and development in the presence of brain-derived growth factor (BDNF) [10]. A study by Wills and co-workers also presented an interesting and unique role for ShcD in promoting EGFR phosphorylation in a ligand-independent manner [6]. Notably,

Abbreviation: Akt,, Protein kinase B;; ALK,, Anaplastic Lymphoma Kinase; CMV,, Cytomegalovirus; DMEM,, Dulbecoo Modified Eagle's Medium;; DNA,, Deoxyribonucleic Acid; ECL,, Enhanced Chemiluminescence;; EGF,, Epidermal Growth Factor;; EGFR,, Epidermal Growth Factor Receptor;; ERK,, Extracellular Signal–Regulated Kinases;; FBS,, Fetal Bovine Serum; FGFR,, fibroblast growth factor receptors; GDNF,, Glial Cell Line-Derived Neurotropic Factor;; GFLs,, GDNF Family Ligands;; GFP,, Green Fluorescent Protein; GPCR,, G-Protein Coupled Receptor; GRB2,, Growth Factor Receptor-Bound Protein 2;; HGFR,, hepatocyte growth factor receptor;; HRP,, Horseradish Peroxidase; hrs,, Hours; IGF,, Insulin Growth Factor;; LB,, Luria-Bertani; mAb,, Monoclonal Antibody; MAP,, Mitogen-Activated Protein;; MAPK,, Mitogen-Activated Protein Kinases; min,, Minute; MuSK,, Muscle Specific Kinase; NFDM,, Non-Fat Dry Milk; PBS,, Phosphate-Buffered Saline; PBST,, Phosphate-Buffered Saline Tween; PDGF,, Platelet-Derived Growth Factor;; PI3K,, Phosphoinositide 3-Kinase; PMSF,, Phenylmethylsulfonyl Fluoride; pAb,, Polyclonal Antibody; pTyr,, Phospho-Tyrosine; PVDF,, Polyvinylidene Fluoride; RET,, Rearranged During Transfection; rpm,, revolution per minute;; RT,, Room Temperature;; RTKs,, Receptor Tyrosine Kinase; SDS-PAGE,, Sodium Dodecylsulphate Polyacrylamide Gel Electrophoresis; ShcD,, Src Homology And Collagen D; Src,, Proto-Oncogene Tyrosine-Protein Kinase Src; TKRs,, Tyrosine Kinase Receptor;; TrkA/B/C,, Tropomyosin-Related Kinase Receptor A/B/C

* Corresponding author.
E-mail address: samahmed@sharjah.ac.ae (S.B.M. Ahmed).
[1] These authors have equally contributed to the work.

https://doi.org/10.1016/j.bbrep.2018.01.007
Received 28 July 2017; Received in revised form 2 January 2018; Accepted 11 January 2018
Available online 28 January 2018

the data have not revealed the exact downstream consequence of the ShcD-receptor association with known interacting receptors.

In an unpublished study, Fagiani demonstrated that ShcD is expressed by neural crest-derived cancers, such as gliomas and neuroblastomas [5]. Additionally, RET tyrosine kinase receptor is essential for neuronal development [11,12]; it has also been shown to promote neuroblastoma prosurvival signalling and migration [13,14]. Another study by Smith and colleagues showed that RET and ShcD associate at the exogenous level in human embryonic kidney cells [8], though no further experiments were performed to elucidate the functional impact of this interaction.

The RET (rearranged during transfection) receptor is one of the tyrosine kinase receptor which is critical for normal development and wellbeing of different cell types [15]. RET is a single-pass transmembrane and similar to the other TKRs, RET possess an extracellular domain, an intracellular domain and a transmembrane membrane region. The RET signalling is triggered through the binding of glial cell line-derived neurotropic factor (GDNF) family ligands (GFLs), which includes GDNF, artemin (ARTN), neurturin (NRTN) and persephin (PSPN) [16].

Based on these observations, further study is needed to decipher the role of the molecular interaction between ShcD and RET in neuroblastoma cells since the role of RET in neuronal cell migration and survival is well determined [16]. In addition, we aimed to explore the effect of this association on downstream signalling and its effects on cellular biological responses, particularly survival and migration.

2. Materials and methods

2.1. Plasmids, antibodies, and growth factors

A full-length clone DNA of the *Homo Sapiens* RET proto-oncogene transcript variant 2 with a C-terminal MYC tag, GFP construct and MYC-tag negative construct were obtained from Sino Biological, Inc, China. GFP-ShcD and empty vector constructs were provided by Dr. Sally A. Prigent, University of Leicester, UK and described previously by Ahmed and Prigent [17].

The glial derived neurotrophic factor (GDNF) from Sigma-Aldrich, UK was prepared in sterile, molecular-grade water to a concentration of 20 μg/ml.

The following primary antibodies were used for immunoblotting, immunoprecipitation and immunofluorescence: anti-RET (sc-9996; Santa Cruz, USA), anti-MYC (ab9106; Abcam, UK), anti-MYC tag (ab18185; Abcam), anti-phospho-tyrosine (ab179530; Abcam), anti-ShcD (sc-165482; Santa Cruz, USA), anti-AKT1/2/3 (ab179463; Abcam), anti-phospho-AKT1/2/3 (sc-7985; Santa Cruz), anti-PKC (ab179522; Abcam), anti-GFP (sc-9996; Santa Cruz), anti-phospho-RET (sc-20252; Santa Cruz), anti-ERK1/2 (9102S; Cell Signalling), anti-phospho-ERK1/2 (4370S; Cell Signalling), anti-β actin (4970S; Cell Signalling), anti-GAPDH (ab37168; Abcam), anti-RET (ab134100; Abcam) and anti-RAB7 (ab198337). Horseradish peroxidase-conjugated anti-goat (ab97023, Abcam), anti-mouse (7076S; Cell Signalling) and anti-rabbit (7074S; Cell Signalling) secondary antibodies were used for immunoblotting. Donkey anti-rabbit IgG Alexa Fluor 647 and goat anti-mouse IgG Alexa Fluor 405 from Abcam were used for immunostaining.

2.2. Cell culture, transfection and GDNF treatment optimization

The neuroblastoma cell line SK-N-AS was obtained from ECACC (Sigma-Aldrich, UK). The cells were maintained at 5% CO_2 and 37 °C in DMEM supplemented with 10% foetal bovine serum (FBS), 1 mM MEM non-essential amino acids, 5 mM L-glutamine and 1% penicillin/streptoMYCin (P/S). For co-immunoprecipitation, cells were seeded in 100-mm culture dishes with 10 ml of media. For the immunofluorescence analysis and wound healing assay, cells were seeded on sterile glass coverslips in 6-well plates with 2 ml of media. For the MTT and caspase 3/7 assays, cells were seeded in 96-well plates with 200 μl of complete media. The cells were transfected with 2 μg of control vector (FLAG-HIS empty vector) as mock transfection, GFP, MYC tag negative vector, GFP-ShcD, MYC-RET or co-transfected with GFP-ShcD and MYC-RET plasmid DNA following the TurboFect manufacturer's guide (Thermo Fisher Scientific; R0531). The same amount of DNA was used for transfection in the case of the individual transfection of GFP, MYC, GFP-ShcD or MYC-RET; the control vector was used to equalize the amount. After transfection, the cells were starved with DMEM containing 0.1% FBS for 4 h and treated with 200 ng/ml for 40 min for the downstream signalling dissection experiment. While for the wound migration the cells were untreated or treated with 200 ng/ml GDNF for 24 h in 10% FBS containing medium. In the assessment of cell viability experiments, the cells were either kept in 1% FBS containing medium or in % FBS containing medium with 200 ng/ml GDNF for 48 h.

2.3. Cell lysate preparation and immunoprecipitation

Following GDNF treatment, cells were washed twice with ice-cold PBS and lysed using pre-chilled Triton lysis buffer containing 1% Triton lysis buffer (50 mM Tris-HCl pH 7.4, 150 mM NaCl, 1 mM EDTA, 1% TritonX-100), 50 mM NaF, 1 mM Na3VO4, 1 mM PMSF and 2% protease inhibitors. The cell lysates were centrifuged at 14,000 rpm for 10 min at 4 °C to remove the cell debris. The protein analysis was performed using a Thermo Scientific Pierce BCA Protein Assay Kit. The sample buffer (3× SB, 100 mM DTT) was then added to the cell lysate of each sample. The samples were stored at (−20 °C). The next day, the samples were heated at 95 °C for 5 min and resolved on an SDS-PAGE gel.

For co-immunoprecipitation, a 25-μl slurry of protein G-sepharose beads (Sigma-Aldrich, UK; P3296) was conjugated with 2–5 μg of the primary antibody and/or control antibody. After immobilizing the antibodies with beads, ~ 500 μl of the cell lysate was added to the beads and kept for incubation at 4 °C for 2 h with gentle rocking. After the incubation, the beads were washed 4 times with 500 μl of washing buffer (1% Triton lysis buffer, 1 mM PMSF, 50 mM NaF and 1 mM Na_3VO_4); 50 μl of the sample buffer (3× SB, 70 mM DTT) was added to the bead pellet and incubated at 95 °C for 5 min immediately before gel loading.

2.4. Immunoblotting

Whole cell lysates (WCLs) or immunoprecipitates were separated on 8–10% SDS-PAGE gels and transferred to polyvinylidene fluoride membranes (Immobilon-P) using a semidry Turbo Transfer system (Bio-Rad). Membranes were blocked in 5% BSA or NFDM in Tris-buffered saline/Tween-20 (TBST) for 1 h. Then, the membrane was incubated with the primary antibody overnight at 4 °C. After incubation, the membranes were washed 4 times with TBST for 10 min each with agitation. The secondary antibody coupled to HRP was diluted in the same blocking buffer for 1 h at room temperature. The membrane was washed 4 times with TBST, and the bands were visualized using ECL chemiluminescence detection reagent (Thermo Scientific Pierce; PL209759A).

2.5. Immunofluorescence staining, confocal microscopy, and colocalization analysis

After GDNF treatment, the culture medium was aspirated from each glass coverslip, rinsed twice with cold 1× PBS and fixed by incubation with 3.7% (v/v) formaldehyde in PBS for 20 min at RT. The cells were then washed three times with PBS for 1–2 min. Thereafter, the cells were permeabilised with 0.1% Triton X-100 in PBS for 10 min at RT, blocked with 3% BSA in PBS for 30 min-1 h at RT and incubated with the primary antibody at 4 °C overnight. Following incubation, the cells were rinsed with PBS, incubated in a sealed, light-impermeable

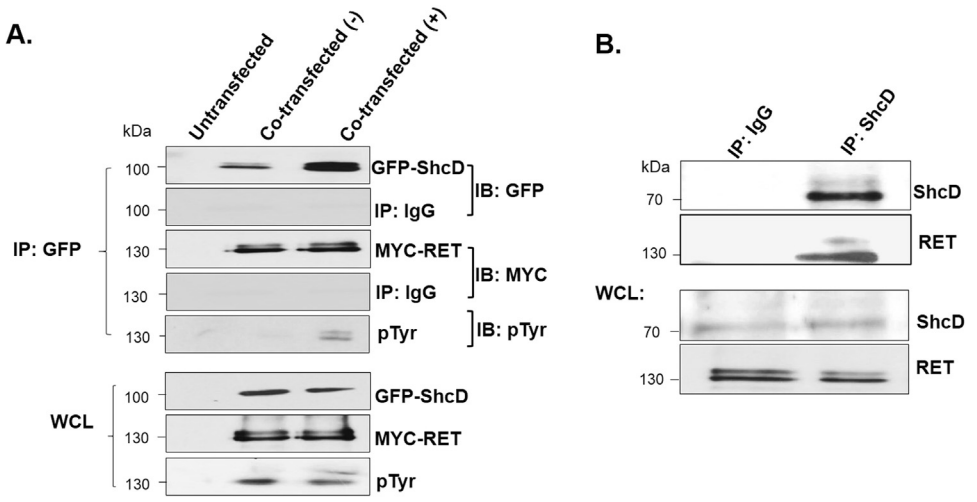

Fig. 1. ShcD co- immunoprecipitated with RET from SK-N-AS cell lysates. (A) SK-N-AS cells were co-transfected with GFP-ShcD and MYC-RET then treated with 200 ng/ml GDNF (+), or left untreated (-). Untransfected, untreated cells were analysed in parallel. Whole cell lysates (WCL) and immunoprecipitates (IP) prepared using anti-GFP antibody or control IgG were RET analysed by SDS-PAGE and immunoblotting (IB) using antibodies to detect GFP, MYC or pTyr (phospho-tyrosine). (B) Endogenous ShcD was immunoprecipitated from untreated SK-N-AS cells and analysed by western blotting with anti-ShcD and anti-RET antibodies.

chamber with the secondary antibody for 1 h at RT, rinsed with PBS, and mounted onto glass slides with antifade mounting medium with DAPI (Abcam; ab104139). The cells were visualized by fluorescence microscopy (Olympus, BX51TF) using cellSens Standard software (version). Colocalization was assessed by merging the resulting images using ImageJ-win64 software.

2.6. MTT assay and caspase-3/7 assay

The SK-N-AS cells were cultured in 96-well plates with a seeding density of 500000 cells per well and transfected as previously described. Following transfection, the cells were starved with DMEM containing 0.1% FBS and incubated for 48 h, followed by GDNF treatment or no treatment. Based on the manufacturer's guide in the MTT kit (Thermo Fisher Scientific; V13154), the medium from each well was removed and replaced with 100 µl of fresh 1% FBS DMEM. Away from the light, 10 µl of the 12 mM MTT stock solution was added into each well and incubated at 37 °C for 4 h. After MTT incubation, 85 µl of medium was removed from each well, and 50 µl of DMSO was added to each well, mixed thoroughly with a pipette, and incubated at 37 °C for 10 min. Thereafter, the absorbance was read at 540 nm. The caspase-3/7 assay was conducted according to the manufacturer's guide (G8090; Promega), and the activity of caspase-3/7 was measured using a microplate reader at an excitation wavelength of 499 nm and an emission wavelength of 521 nm.

2.7. Wound healing assay

Cells were seeded at a high density in 6-well plates before the introduction of plasmid DNA. After transfection, a straight scratch was made in each well using the tip of a 10-µl pipette (keeping the pipette tip under an angle of approximately 30 degrees to maintain a limited scratch width). Then, the medium was removed from the cells, and the cells were washed once with 1 ml of PBS to remove the floating cells. Two millilitres of fresh complete phenol red-free DMEM either with or without GDNF treatment (200 ng/ml) was added to the cells. Thereafter, using a fine marker, the specific position was defined beneath the bottom of each well, and images were acquired at 0, 8, 16, and 24 h. The acquisition of the pictures was performed using an Optika microscope and Optika camera (XDS-2) with a 10× objective, and the analysis was performed using ImageJ-win64 software.

2.8. Statistical analysis

Band intensity quantification was performed using ImageJ-win64 software. The data from the MTT and caspase-3/7 assays were analysed by *t*-test, and a p value < 0.05 was considered statistically significant. Error bars represent the standard error of the mean (SEM). All data analyses were performed using EXCEL 2010. Wound-healing assay analysis was performed with ImageJ-win64 and EXCEL 2010.

3. Results

3.1. The molecular interaction between the recombinant ShcD adaptor protein and RET proto-oncogene in SK-N-AS cells

To investigate the molecular association between ShcD and RET in SK-N-AS cells, co-immunoprecipitation was employed. The cells were either untransfected or transiently co- transfected with GFP-ShcD and MYC-RET and then left untreated or treated with GDNF. Immobilized anti-GFP and anti-IgG antibodies were used for co-immunoprecipitation.

The proteins that were retained on the immobilized antibodies were analysed by SDS-PAGE and immunoblotting with anti-MYC and anti-GFP antibodies. For the anti-GFP immunoprecipitates, bands that corresponded to both GFP-ShcD and MYC-RET were detected in the GDNF-treated and untreated cells, while no similar bands were detected in the IgG immunoprecipitates (Fig. 1, A).

To verify the activation of the RET receptor upon GDNF treatment, the blots were stripped and re-probed with anti-pTyr (phospho-tyrosine) antibody. In the co-transfected cells, phosphorylated RET was observed in the immunoprecipitates of the GDNF-treated cells but not in the untreated cells (Fig. 1, A). These findings showed that GFP-ShcD successfully co-immunoprecipitated with both phosphorylated and unphosphorylated RET.

3.2. The association of ShcD and RET in SK-N-AS at the physiological level

Both ShcD and RET were shown to be abundantly expressed in neuronal tissues and cells [16,18,19]; therefore, co-immunoprecipitation was performed using lysates obtained from untransfected SK-N-AS cells. Endogenous ShcD was immunoprecipitated with anti-ShcD antibody, and the associated endogenous RET was detected by immunoblotting with anti-RET antibody (Fig. 1, B). No similar band was detected with the control antibody. Our results indicated that endogenous ShcD and RET co-immunoprecipitated from the SK-N-AS neuroblastoma cell lysate without any enhancement from the overexpression system or GDNF treatment.

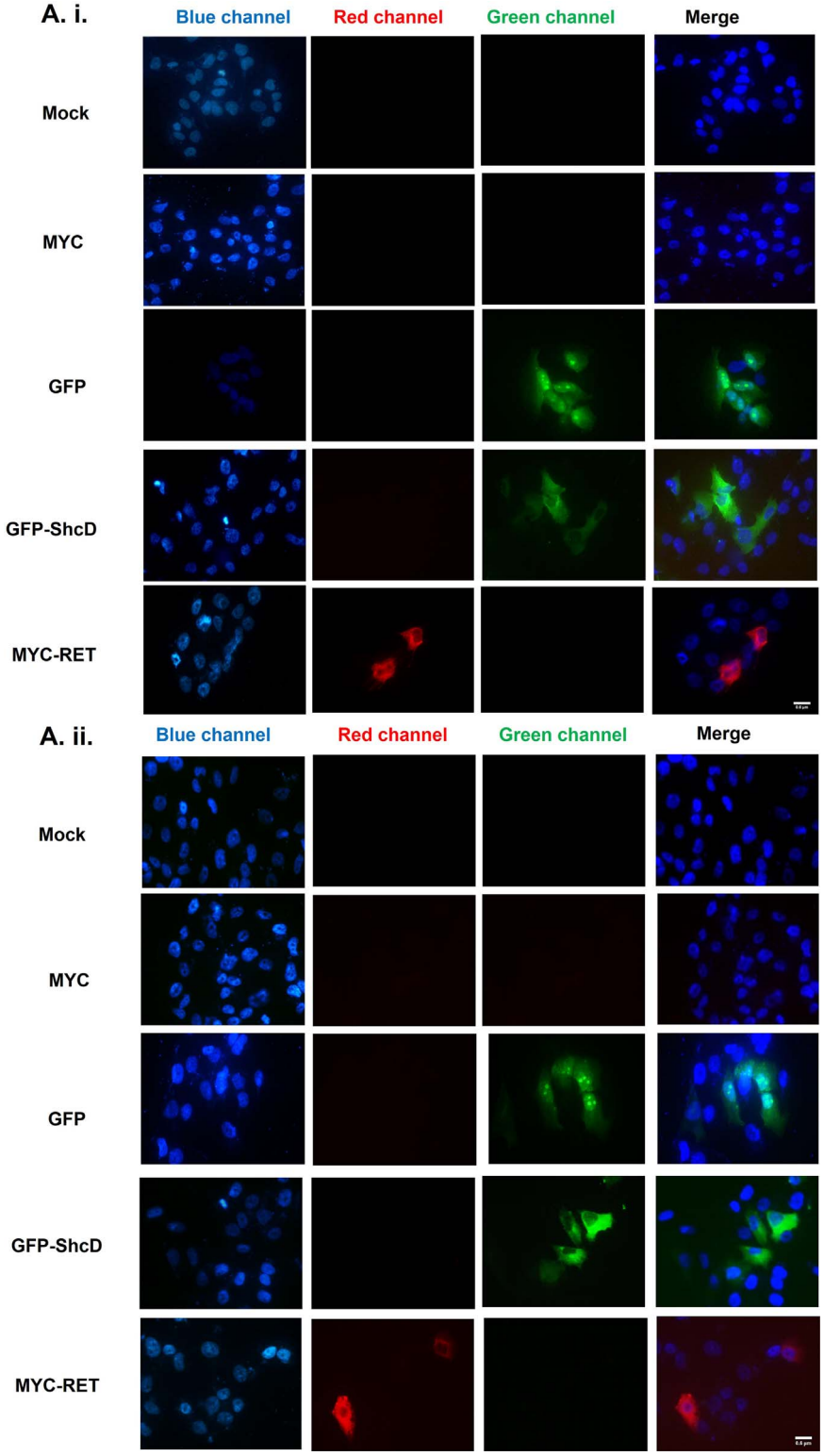

Fig. 2. Subcellular colocalization of ShcD and RET in SK-N-AS cells. (A) SK-N-AS cells were seeded on coverslips and transfected with either empty vector (mock transfection), MYC-tag vector, GFP, GFP-ShcD or MYC-RET. After 24 h, cells were untreated (A.i) or treated (A.ii) with 200 ng/ml GDNF for 40 min. The cells were then fixed and stained with anti-RET antibody (red channel) to analyse the subcellular distribution of GFP-ShcD and MYC-RET individually. GFP and GFP-ShcD were detected at the green channel. (B & C) The SK-N-AS cells on coverslips were co-transfected with GFP and MYC-tag vector or MYC-RET and GFP-ShcD. After 24 h, cells were either untreated (B. i) or treated (B. ii) with 200 ng/ml GDNF for 40 min. Then, cells were fixed and analysed by fluorescence microscopy. (D) Endosomal colocalization of GFP-ShcD and MYC-RET in co-transfected and GDNF-treated cells was detected by staining with anti-Rab7 antibody, a late-endosome marker. The cells were visualized by fluorescence microscopy (Olympus, BX51TF) with a 60× objective using cellSens Standard software. The merge represents the overlay of the red, green and blue channels. The overlay performed using ImageJ-win64 software. The white arrows indicate the regions of interest. Scale bar = 0.6 μm. (For interpretation of the references to color in this figure legend, the reader is referred to the web version of this article.)

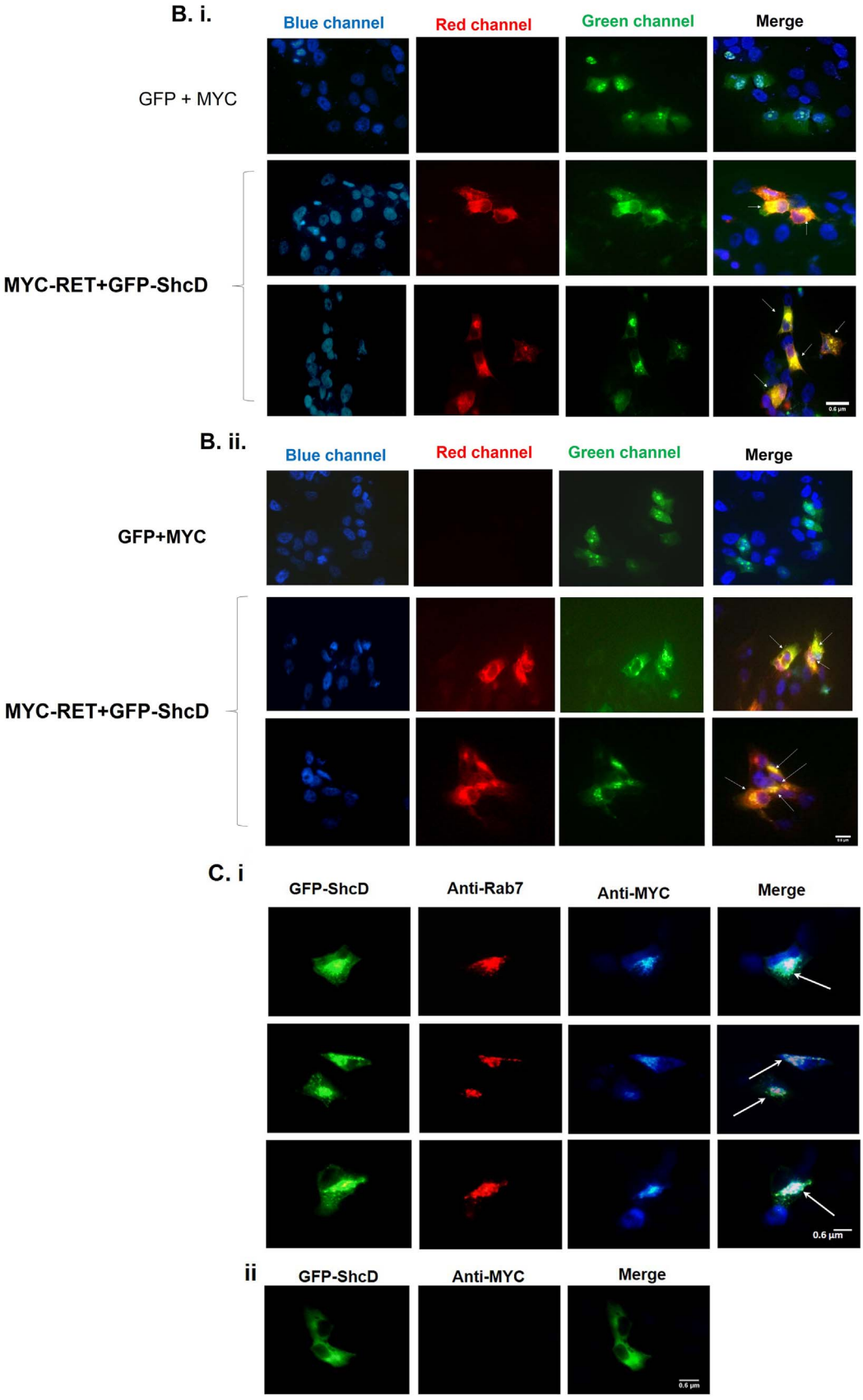

Fig. 2. (*continued*)

3.3. Subcellular colocalization of the ShcD adaptor protein with the RET receptor

To further validate the ShcD-RET association, their subcellular co-localization was validated by immunofluorescence. The SK-N-AS cells were transfected with empty vector (mock transfection), GFP, MYC-tag vector, GFP-ShcD or MYC-RET constructs individually, while another set of cells were co-transfected with GFP and MYC or GFP-ShcD and MYC-RET constructs. The GDNF treatment was applied to one set of the samples (Fig. 2, Aii), and the other set was left untreated (Fig. 2, Ai). The cells were fixed, permeabilized, and immunolabelled with anti-RET antibody.

Similar to GFP-ShcD, MYC-RET demonstrated a uniform cytoplasmic distribution when it was transfected individually in the SK-N-AS without and with GDNF treatment (Fig. 2, Ai, ii). However, GFP-ShcD and MYC-RET coexpression in Sk-N-AS cells resulted in their co-localization to an endosome-like structure at the perinuclear region of both untreated and GDNF-treated cells (Fig. 2, Bi, ii). GFP was observed to be distributed through all the cellular compartments with no evident difference upon treating the cells with GDNF or leaving them untreated. Whereas, MYC transfected cells showed no red signal at the red channel upon staining the cells with anti-RET antibody (Fig. 2, Ai, ii).

To identify the subcellular compartment into which ShcD and RET translocate upon coexpression and GDNF treatment, anti-Rab7 (endosome marker) was used. GFP-ShcD and MYC-RET coexpression demonstrated a similar distribution pattern, as shown earlier. Anti-Rab7 (red) revealed that ShcD (green) and RET (blue) translocate to endosomes when they are coexpressed in GDNF-treated cells (Fig. 2, Ci). Since we used anti-MYC antibody to detect MYC-RET, it was crucial to verify that the signal detected in the blue channel was not due to detection of endogenous MYC (Fig. 2, Cii).

3.4. Investigating the impact of the ShcD adaptor protein and RET receptor interaction on downstream signalling pathways

To confirm that the ShcD adaptor protein was one of the intracellular binding partners of the RET receptor, it was necessary to study the impact of the ShcD-RET interaction on ERK and AKT signalling since RET is known to activate both signalling cascades [20–22]. Notably, ShcD has also been shown to increase ERK phosphorylation upon BDNF treatment [10]. The seeded SK-N-AS cells were transfected with either empty vector, GFP, MYC-tag vector, MYC-RET, or GFP-ShcD or co-transfected with GFP-ShcD and MYC-RET (Fig. 3, Ai, ii).

RET phosphorylation was elevated in the GDNF-treated cells, whereas RET and ShcD coexpression yielded a reduction in RET phosphorylation. Mock transfected cells, GFP transfected or MYC-tag transfected cells showed no conspicuous change in phosphorylated ERK or AKT (Fig. 3A ii). The level of phosphorylated ERK was elevated in the GDNF-treated GFP-ShcD-expressing cells compared with the cells that coexpressed GFP-ShcD and RET ($p = 0.06$) (Fig. 3, B). On the other hand, the GDNF-treated MYC-RET-transfected cells showed higher levels of phosphorylated AKT, and the coexpression of both GFP-ShcD and MYC-RET resulted in a reduction in phosphorylated AKT ($p = 0.013$) (Fig. 3, C).

Based on these findings, it was concluded that the coexpression of MYC-RET and GFP-ShcD downregulated ERK and AKT signal transduction in GDNF-treated cells.

3.5. The impact of the ShcD-RET association on SK-N-AS cell viability

Consequent to the observed effect of GFP-ShcD and MYC-RET coexpression in downregulating ERK and AKT activation, the functional effect of the ShcD and RET interaction in SK-N-AS cells was analysed. After the cells were seeded in 96-well plates, they were transfected with either the empty vector, MYC-tag vector, GFP, MYC-RET, or GFP-ShcD or co-transfected with GFP-ShcD and MYC-RET. After 24 h, the cells were treated with either 0.1% Serum or 0.1% Serum and 200 ng/ml GDNF for 48 h. In the cells transfected with MYC-RET, cell viability was found to be significantly higher compared to the cells that were co-transfected with MYC-RET and GFP-ShcD and cells that were treated with GDNF ($p = 0.035 < 0.05$), unlike the GFP-ShcD-transfected cells that showed no significant effect on cell viability (Fig. 4, A). Similarly, the MYC-RET-transfected cells with no GDNF treatment showed slight increase in cell viability than the MYC-RET and GFP-ShcD co-transfected cells with no GDNF treatment ($p = 0.2 > 0.05$).

For a further evaluation of cell viability in GFP-ShcD and MYC-RET-coexpressing SK-N-AS cells, caspase-3/7 assay was conducted using the aforementioned conditions as the cell viability assay to validate apoptosis in SK-N-AS cells upon transfection. Upon GDNF treatment, cells coexpressing GFP-ShcD and MYC-RET exhibited marginally significant increase in caspase-3/7 activity in comparison with MYC-RET-transfected cells ($p = 0.1 > 0.05$) (Fig. 4, B). Likewise, with no GDNF treatment cells coexpressing GFP-ShcD and MYC-RET exhibited less significant increase in caspase-3/7 activity in comparison with MYC-RET-transfected cells ($p = 0.15 > 0.05$) (Fig. 4, B).

In conclusion, the cells coexpressing GFP-ShcD and MYC-RET demonstrated more caspase-3/7 activity compared to the MYC-RET-expressing cells in both GDNF treated and untreated cells with more evident increase with GDNF treatment.

3.6. The influence of ShcD-RET coexpression on SK-N-AS cell migration

Both ShcD and RET were demonstrated to play roles in cell migration [5,14]; therefore, we aimed to study the role of the ShcD-RET interaction in SK-N-AS cell migration. The cells were transfected with the empty vector, MYC-tag vector, GFP, MYC-RET, or GFP-ShcD or co-transfected with GFP-ShcD and MYC-RET. After 24 h, the cells were either untreated or treated with 200 ng/ml GDNF. Thereafter, wound healing assays were conducted, and cell migration was evaluated using an Optika microscope.

Consistent with the reported role of ShcD in mediating melanoma migration, GFP-ShcD-transfected cells demonstrated the highest rate of migration with and without GDNF treatment (Fig. 5, A, B). The GFP-ShcD-mediated cell migration was reduced by GFP-ShcD coexpression with MYC-RET. On the other side, MYC-RET-transfected cells underwent limited migration in the absence of GDNF (Fig. 5, Aii), while the GDNF treatment resulted in enhancement of the cell migration (Fig. 5, Bii). Surprisingly, in the presence of GDNF, the SK-N-AS cells coexpressing GFP-ShcD and MYC- RET showed a remarkable reduction in cell migration compared to their counterparts with no GDNF treatment ($p = 0.04$) (Fig. 5, Aii, Bii).

4. Discussion

The latest identified Shc family member, ShcD, was found to be abundantly expressed in neuronal tissues and invasive melanoma, promoting cellular migration and tumourigenesis [6]. Furthermore, a spot peptide array revealed the interaction between ShcD and different tyrosine kinase receptors, such as MuSK, EGFR, ErbB2 and RET, but the consequence of these interactions is yet to be determined [6,8,9]. To reveal the role of ShcD in neuronal cells, this study aimed to investigate the interaction of the full-length ShcD adaptor protein with the RET receptor and to assess the functional impact of their association since the latter role in neuronal cell migration and survival was well determined [16].

In addition to employing transfected SK-N-AS neuroblastoma cells, co-immunoprecipitation experiments provided clear evidence for a novel ShcD and RET interaction at both exogenous and endogenous levels. The association of ShcD with RET is not an extraordinary finding for Shc family proteins since ShcC has been identified as a physiological substrate of the activated RET oncoprotein, which activates the PI3K/AKT signalling pathway and promotes cancer cell survival [21].

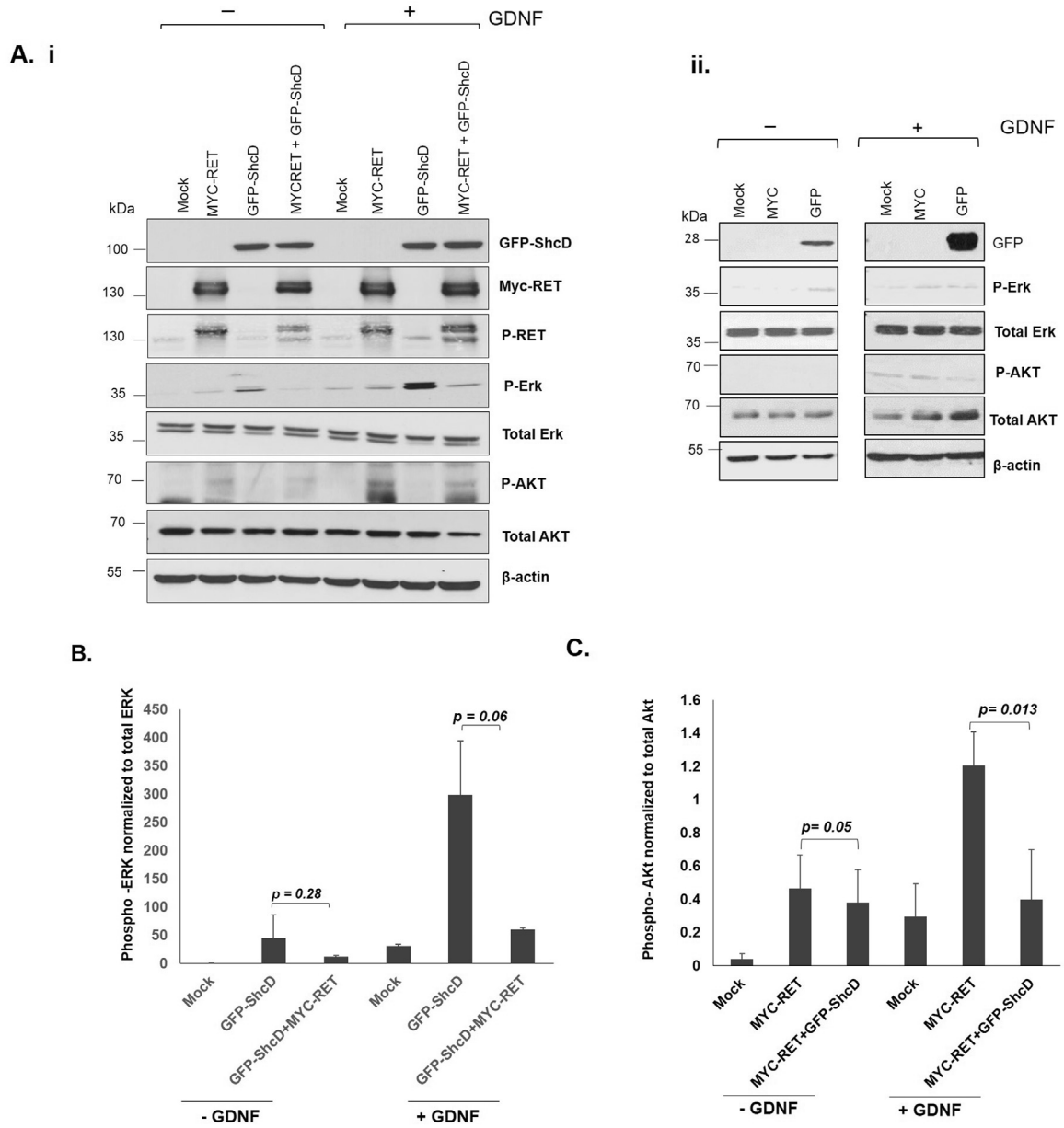

Fig. 3. Western blotting showing the impact of the ShcD adaptor protein and RET receptor interaction on the downstream signalling pathways. (A) The SK-N-AS cells were transfected with the empty vector (mock transfection), MYC-tag vector, GFP, MYC-RET, GFP-ShcD or co-transfected with GFP-ShcD and MYC-RET. Cells were starved for 6 h and either treated with 200 ng/ml GDNF for 40 min, or left untreated. The cell lysates were resolved on 10% SDS-PAGE gels. Western blotting was performed using anti-GFP, anti- MYC, anti-phospho-RET, anti-pErk1/2, anti-Erk1/2, anti-pAkt1/2/3, anti-Akt1/2/3 and anti-β-actin antibodies. (B) Densitometry analysis of immunoblots. The results are representative of three independent experiments. Densitometry was performed using ImageJ-win64 software. (i) The graph shows the ratio of p-Erk to total Erk ($p = 0.28^{<}0.05$) ($p = 0.06^{<}0.05$). (ii) The graph shows the ratio of p-Akt to total Akt ($p=0.05$) ($p=0.013^{<}0.05$). Error bars represent the SEM.

Unlike the study by Smith and co-workers which showed the interaction of ShcD with RET in HEK 293 embryonic kidney cells at the exogenous level only [8], for the first time, we were able to show that the interaction of full-length ShcD with RET occurs in GDNF-treated and untreated neuroblastoma cells and appears at both endogenous and exogenous levels.

The ShcD-RET association was validated by studying their co-localization using immunofluorescence. Interestingly, when coexpressed, ShcD and RET accumulated at a perinuclear endosome-like compartment that also showed positive staining for the late endosomal marker. Based on these data, it was inferred that ShcD promotes RET internalization with and without GDNF treatment. GDNF treatment was previously shown to provoke RET internalization [23], which indeed supports the endosomal colocalization of ShcD and RET in GDNF-treated cells. Ina addition, a recent report by Will and et al. showed that ShcD colocalizes with EGFR at the perinuclear endosomal compartment [24].

The ShcA-RET association mediates the internalization of the RET receptor via endocytosis, and the fate of the internalized receptor can be either recycling or degradation, which is mainly determined by the assembly of different adaptor proteins [25]. Notably, the ShcA protein was also found to mediate EGFR internalization in a ligand-dependent manner [26,27]. As a consequence of ShcD-mediated RET internalization, the phosphorylation of RET is predictably reduced because fewer RET proteins are available on the cell surface to bind GDNF.

Intriguingly, the ShcD-RET association was found to have a distinct unexpected role in the signalling cascades of SK-N-AS neuroblastoma cells. RET overexpression was shown to promote AKT activation, which is consistent with previous reports, however coexpression with ShcD inhibited this activation in the presence of GDNF. Similarly, ShcD-

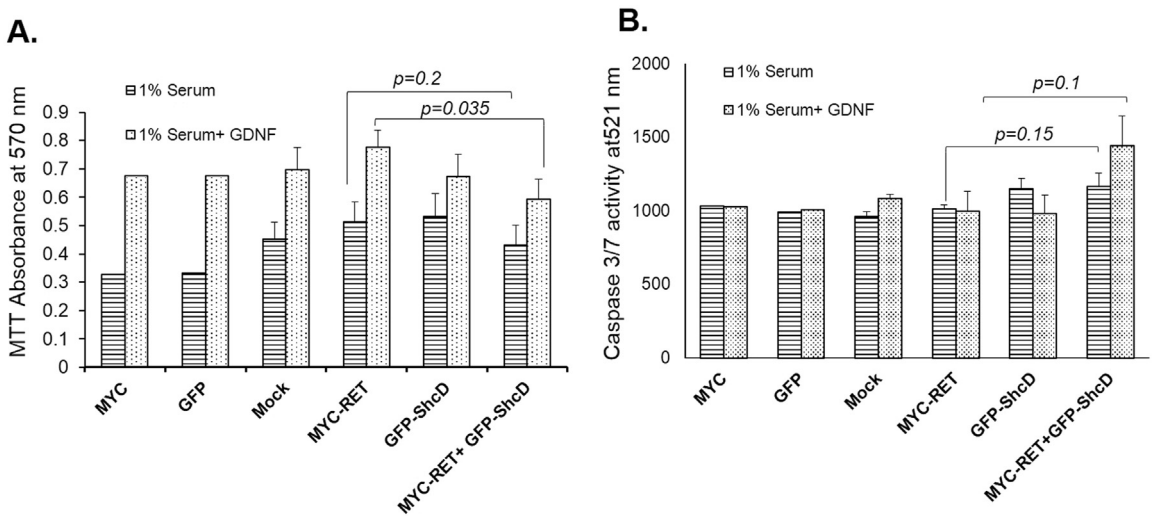

Fig. 4. Effect of GFP-ShcD and MYC-RET co-expression on SK-N-AS cell viability and apoptosis. SK-N-AS cells were transfected with the empty vector (mock transfection), MYC-tag vector, GFP, MYC-RET, GFP-ShcD or co-transfected with GFP-ShcD and MYC-RET. After 24 h, medium contained 1% serum with or without either 200 ng/ml GDNF was added to the cells for 48 h. The cell viability was measured by MTT assay. (A) The absorbance reading of the assay was measured using a microplate reader at 540 nm. ($p = 0.034 < 0.05$). The caspase-3/7 activity, which reflects the induction of apoptosis in the SK-N-AS cells (B), was measured using a microplate reader at an excitation wavelength of 499 nm and an emission wavelength of 521 nm ($p = 0.1 > 0.05$) ($p = 0.15 < 0.05$). Error bars represent the SEM.

mediated ERK phosphorylation was reduced when ShcD was coexpressed with RET in GDNF-treated cells. In contrast to the role of the Shc proteins in activation of downstream signalling pathways, our data showed that the RAS/ERK and PI3K/AKT pathways were downregulated in GDNF-treated SK-N-AS neuroblastoma cells upon coexpression of ShcD and RET. Notably, the RAS/ERK pathway was found to be inhibited by p66ShcA upon IGF-1 receptor stimulation [28,29]. Furthermore, the confirmed enrolment of ShcD as a substrate for other receptors, such as TrkB [10], could justify the ability of ShcD to activate the RAS/ERK pathway in SK-N-AS overexpressing the ShcD protein with no GDNF treatment. While this manuscript was in preparation a study by Wills and colleagues revealed that ShcD deactivates ERK and AKT signalling downstream of RET and TrkB, which certainly concurs with our finding [30]; nevertheless, their data do not reveal the consequence of the inhibition.

In contrast to the role of ShcC in activating the PI3K/AKT signalling pathway [21], AKT phosphorylation was found to be suppressed in the GDNF-treated SK-N-AS cells overexpressing ShcD and RET compared with the untreated cells.

Consistent with the role of RET in cell survival [16], RET enhanced cell viability in GDNF-treated SK-N-AS, in comparison to serum-starved cells, while unexpectedly, its coexpression with ShcD reduced cell viability. The activation of RET by GDNF is known for its role in the proliferation and viability of neuroblastoma [31,32]. Moreover, RET was shown to mediate enteric neuroblast cell death via caspase activation [33].

Upon GDNF treatment, the migration ability of ShcD-overexpressing cells was enhanced, which is consistent with the role of ShcD in melanoma migration [5]. However, its coexpression with RET dramatically reduced SK-N-AS migration following GDNF treatment. The observed endosomal colocalization of both RET and ShcD explained the detected reduction in cell viability and motility. It was deduced that ShcD sequestered RET in the endosomes and in so doing, it acted as a molecular switch that could turn off downstream signalling pathways, particularly the ERK/MAPK and PI3K/AKT pathways, upon its association with the RET receptor (Fig. 6). The same phenomenon was observed with ShcA in partitioning the TGF-β receptor complex from the plasma membrane to the endosomal compartment [34].

This multi-faceted property of ShcD is not novel in regard to Shc proteins, as p66Shc (an isoform of ShcA) was reported to induce apoptosis upon oxidative stress [29,35], while in other studies, it was found to promote nodal metastasis in breast cancer patients [36]. Additionally, a report by Micol Ferro and others demonstrated an inhibitory role for ShcC in downregulating T cell antigen receptor signalling [37].

5. Conclusion

In this study, we were able to identify a new role for the melanoma-associated Shc adaptor ShcD in internalizing the RET receptor that negatively affected cell viability and motility of neuroblastoma cells. The data suggest a switching role for ShcD that relies on the type of cancer and the context of ShcD coexpression with other oncogenes. In addition, our findings might also indicate that the proposal of ShcD as a potential therapeutic target is yet to be determined since its tumour suppressor property was shown in this report.

Acknowledgments

Our sincere thanks go to Keerthi Rajan for her technical help in some of the experiments.

Conflict of interest

The authors declare no conflicts of interest.

Limitations

The co-transfection system is not the most accurate system to dissect signalling pathways, but the problem we are facing with ShcD is the lack of commercially trusted ShcD antibody.

Funding

This project was partly funded by Al Jalila Foundation, Dubai-UAE (project No AJF201636) for providing the funds to carry out this project and Environment and Cancer group funding, Sharjah institute for medical research, University of Sharjah, UAE.

Contributions

Zeanap A. Mabruk: Performed the experiments and participated in

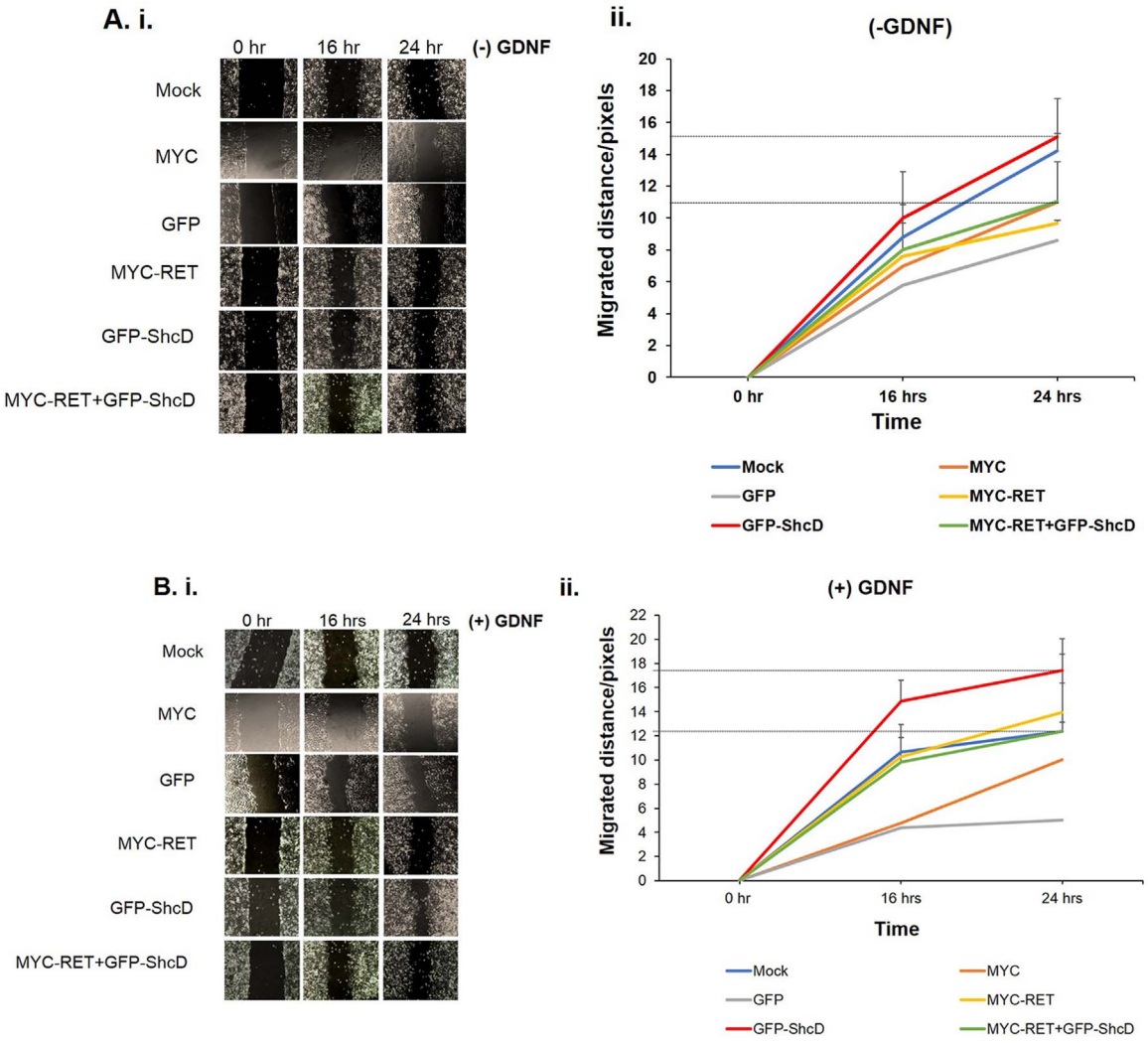

Fig. 5. Wound-healing assay to study migration of the GFP-ShcD and MYC-RET co- transfected SK-N-AS cells. The images and the multiline charts represent the wound-healing rates, which reflect the migration capability of the SK-N-AS cells transfected with the empty vector (mock transfection), MYC-tag vector, GFP, MYC-RET, GFP-ShcD or co-transfected with GFP-ShcD and MYC-RET. The cells were either untreated (A) or treated with 200 ng/ml GDNF (B). The wound healing at a marked position of the scratch was monitored at 0,16, and 24 h using an Optika microscope. The acquisition of pictures was carried out using an Optika camera (XDS-2) with a 10× objective. The analysis was performed using ImageJ-win64 software.

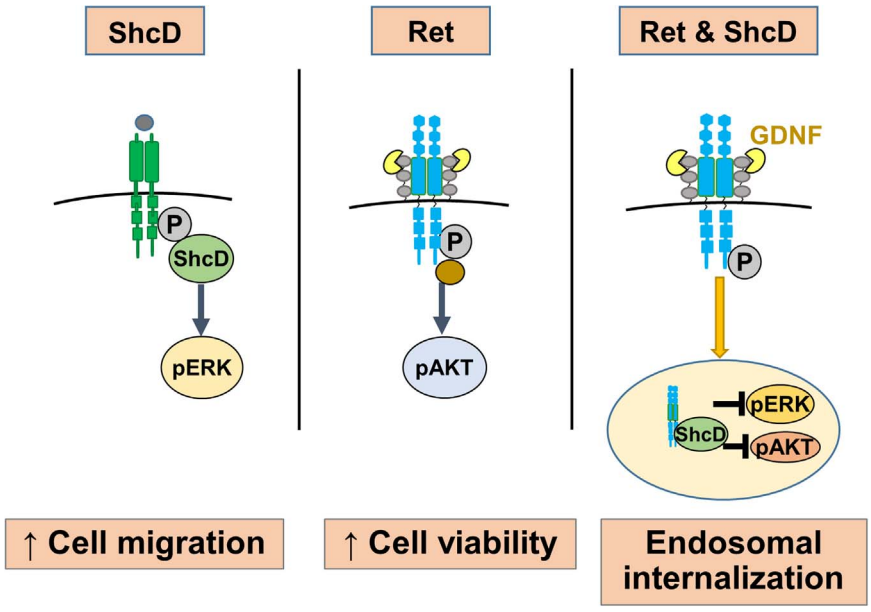

Fig. 6. Schematic presentation demonstrates and summarizes the consequence of ShcD-RET association in neuroblastoma.

writing the manuscript.

Samrein BM Ahmed: Supervised the work, designed the experiments, performed some of the experiments, analysed the data, and participated in writing the manuscript.

Sally A Prigent: Preliminary experiments identifying RET in ShcD complexes were initiated in SAP's lab. Provided GFP-ShcD and the empty vector construct and proofread the manuscript.

Asha Caroline: Technical assistance.

References

[1] D.C. Flynn, Adaptor proteins, Oncogene 20 (44) (2001) 6270–6272.
[2] K.M. Suen, et al., Interaction with Shc prevents aberrant Erk activation in the absence of extracellular stimuli, Nat. Struct. Mol. Biol. 20 (5) (2013) 620–627.
[3] M.K. Lee, et al., TGF-beta activates Erk MAP kinase signalling through direct phosphorylation of ShcA, EMBO J. 26 (17) (2007) 3957–3967.
[4] E. Woldt, et al., Differential signaling by adaptor molecules LRP1 and ShcA regulates adipogenesis by the insulin-like growth factor-1 receptor, J. Biol. Chem. 286 (19) (2011) 16775–16782.
[5] E. Fagiani, et al., RaLP, a new member of the Src homology and collagen family, regulates cell migration and tumor growth of metastatic melanomas, Cancer Res. 67 (7) (2007) 3064–3073.
[6] M.K. Wills, et al., The ShcD signaling adaptor facilitates ligand-independent phosphorylation of the EGF receptor, Mol. Biol. Cell 25 (6) (2014) 739–752.
[7] L. Pasini, et al., Melanoma: targeting signaling pathways and RaLP, Expert Opin. Ther. Targets 13 (1) (2009) 93–104.
[8] M.J. Smith, et al., Screening for PTB domain binding partners and ligand specificity using proteome-derived NPXY peptide arrays, Mol. Cell. Biol. 26 (22) (2006) 8461–8474.
[9] N. Jones, et al., Analysis of a Shc family adaptor protein, ShcD/Shc4, that associates with muscle-specific kinase, Mol. Cell. Biol. 27 (13) (2007) 4759–4773.
[10] Y. You, et al., ShcD interacts with TrkB via its PTB and SH2 domains and regulates BDNF-induced MAPK activation, BMB Rep. 43 (7) (2010) 485–490.
[11] L. Li, et al., The role of RET receptor tyrosine kinase in dopaminergic neuron development, Neuroscience 142 (2) (2006) 391–400.
[12] P. Soba, et al., The RET receptor regulates sensory neuron dendrite growth and integrin mediated adhesion, Elife 4 (2015).
[13] P.E. Zage, C.U. Louis, S.L. Cohn, New aspects of neuroblastoma treatment: ASPHO 2011 symposium review, Pediatr. Blood Cancer 58 (7) (2012) 1099–1105.
[14] X. Ding, et al., Vandetanib-induced inhibition of neuroblastoma cell migration and invasion is associated with downregulation of the SDF-1/CXCR4 axis and matrix metalloproteinase 14, Oncol. Rep. 31 (3) (2014) 1165–1174.
[15] M.A. Lemmon, J. Schlessinger, Cell signaling by receptor tyrosine kinases, Cell 141 (7) (2010) 1117–1134.
[16] L.M. Mulligan, RET revisited: expanding the oncogenic portfolio, Nat. Rev. Cancer 14 (3) (2014) 173–186.
[17] S.B. Ahmed, S.A. Prigent, A nuclear export signal and oxidative stress regulate ShcD subcellular localisation: a potential role for ShcD in the nucleus, Cell Signal 26 (1) (2014) 32–40.
[18] E. Cattaneo, P.G. Pelicci, Emerging roles for SH2/PTB-containing Shc adaptor proteins in the developing mammalian brain, Trends Neurosci. 21 (11) (1998) 476–481.
[19] S.P. Hawley, et al., Expression patterns of ShcD and Shc family adaptor proteins during mouse embryonic development, Dev. Dyn. 240 (1) (2011) 221–231.
[20] R.M. Melillo, et al., The insulin receptor substrate (IRS)−1 recruits phosphatidylinositol 3-kinase to Ret: evidence for a competition between Shc and IRS-1 for the binding to RET, Oncogene 20 (2) (2001) 209–218.
[21] G. Pelicci, et al., The neuron-specific Rai (ShcC) adaptor protein inhibits apoptosis by coupling RET to the phosphatidylinositol 3-kinase/Akt signaling pathway, Mol. Cell. Biol. 22 (20) (2002) 7351–7363.
[22] G.R. Panta, et al., Direct phosphorylation of proliferative and survival pathway proteins by RET, Surgery 138 (2) (2005) 269–274.
[23] D.S. Richardson, A.Z. Lai, L.M. Mulligan, RET ligand-induced internalization and its consequences for downstream signaling, Oncogene 25 (22) (2006) 3206–3211.
[24] M.K.B. Wills, H.R. Lau, N. Jones, The ShcD phosphotyrosine adaptor subverts canonical EGF receptor trafficking, J. Cell Sci. (2017).
[25] D.S. Richardson, et al., Alternative splicing results in RET isoforms with distinct trafficking properties, Mol. Biol. Cell 23 (19) (2012) 3838–3850.
[26] M.P. Oksvold, et al., Immunocytochemical localization of Shc and activated EGF receptor in early endosomes after EGF stimulation of HeLa cells, J. Histochem. Cytochem. 48 (1) (2000) 21–33.
[27] K. Sakaguchi, Y. Okabayashi, M. Kasuga, Shc mediates ligand-induced internalization of epidermal growth factor receptors, Biochem. Biophys. Res. Commun. 282 (5) (2001) 1154–1160.
[28] G. Xi, X. Shen, D.R. Clemmons, p66shc negatively regulates insulin-like growth factor I signal transduction via inhibition of p52shc binding to Src homology 2 domain-containing protein tyrosine phosphatase substrate-1 leading to impaired growth factor receptor-bound protein-2 membrane recruitment, Mol. Endocrinol. 22 (9) (2008) 2162–2175.
[29] S.S. Bhat, D. Anand, F.A. Khanday, p66Shc as a switch in bringing about contrasting responses in cell growth: implications on cell proliferation and apoptosis, Mol. Cancer 14 (2015) 76.
[30] M.K. Wills, et al., Signalling adaptor ShcD suppresses Erk phosphorylation distal to the RET and Trk neurotrophic receptors, J. Biol. Chem. (2017).
[31] H. Futami, R. Sakai, RET protein promotes non-adherent growth of NB-39-nu neuroblastoma cell line, Cancer Sci. 100 (6) (2009) 1034–1039.
[32] L.L. Stafman, E.A. Beierle, Cell Proliferation in Neuroblastoma, Cancers 8 (2016).
[33] M.C. Bordeaux, et al., The RET proto-oncogene induces apoptosis: a novel mechanism for Hirschsprung disease, EMBO J. 19 (15) (2000) 4056–4063.
[34] B.P. Muthusamy, et al., ShcA protects against epithelial-mesenchymal transition through compartmentalized inhibition of TGF-beta-induced Smad activation, PLoS Biol. 13 (12) (2015) e1002325.
[35] M. Pellegrini, et al., p66SHC promotes T cell apoptosis by inducing mitochondrial dysfunction and impaired Ca2+ homeostasis, Cell Death Differ. 14 (2) (2007) 338–347.
[36] J.G. Jackson, et al., Elevated levels of p66 Shc are found in breast cancer cell lines and primary tumors with high metastatic potential, Clin. Cancer Res. 6 (3) (2000) 1135–1139.
[37] M. Ferro, et al., The Shc family protein adaptor, Rai, negatively regulates T cell antigen receptor signaling by inhibiting ZAP-70 recruitment and activation, PLoS One 6 (12) (2011) e29899.